

PACS numbers: 52.38.Ph; 52.59.Ye; 42.65.Re
DOI: 10.1070/QE2013v043n05ABEH015040

Generation of intense coherent attosecond X-ray pulses using relativistic electron mirrors*

V.V. Kulagin, V.N. Kornienko, V.A. Cherepenin, H. Suk

Abstract. **We analyse the steepening of the leading edge of femtosecond petawatt pulses with the use of plasma layers and show that, at an electron density several times higher than the critical one, an asymmetric (in time domain) pulse can be produced with an amplitude of the first half-wave differing little from the maximum pulse amplitude. Using numerical simulation, we have studied the interaction of such pulses with nanometre-thick films, including the generation of relativistic electron mirrors and the reflection of a counterpropagating probe pulse from such mirrors. The resulting coherent X-ray pulses have a duration of ~120 as and a power of ~600 GW at a wavelength of ~13 nm. Our results demonstrate that the reflectivity of a relativistic electron mirror situated in the accelerating pulse field is independent of the probe pulse amplitude when it increases up to the accelerating pulse amplitude.**

Keywords: *generation of coherent attosecond X-ray pulses, very intense nonadiabatic laser pulses, relativistic electron mirrors.*

1. Introduction

There is currently an immense need for a high-power, compact source of short X-ray pulses. Coherent attosecond X-ray pulses may find very wide application in the visualisation of dynamic states of complex molecules, medical diagnostics etc. One way of generating short X-ray pulses is by using Thomson scattering of photons by counterpropagating relativistic electrons. This process, however, usually produces incoherent X-ray pulses. For the generation of coherent X-ray pulses, the electron beam should have a rather small spatial length. At present, single electron bunches moving at a relativistic velocity and having a density approaching the electron density in solids can be produced using modern petawatt laser systems generating pulses several tens of femtoseconds in duration [1, 2]. Necessary conditions for this are a nonadiabatic laser pulse shape (i.e. the pulse leading edge should be shorter than the field oscillation period) and a sufficient pulse amplitude, exceeding a certain threshold. For example, when such a pulse is normally incident on a nanometre-thick film (nanofilm), it can expell all the electrons from the film in the pulse propagation direction. As a result, the electrons acquire relativistic velocities in a time considerably shorter than the laser field period. The spatial length of the electron bunches thus produced may be several nanometres. At electron velocities approaching the speed of light in vacuum, this corresponds to an electron beam duration of about several tens of attoseconds. The bunch diameter is of the order of several tens of microns (laser focal spot diameter), which considerably exceeds the bunch thickness. As a result, such bunches can be used as relativistic electron mirrors.

At present, the main obstacle to the practical implementation of the idea of producing relativistic electron mirrors using nanofilms is the insufficient slope of the leading edge of accelerating laser pulses. At a low slope of the pulse leading edge, the electron bunch lifetime is not very long or no bunches are formed at all. One possible approach for increasing the leading edge slope is to employ the steepening of a petawatt laser pulse when it interacts with solid nanofilms [3–5]. The ability to produce laser pulses of desired shape with the use of nanofilms relies on relativistic nonlinearity and self-induced transparency effects [6–12]. The steepening of the leading edge of an incident laser pulse is due to the following physical mechanism: When the wave amplitude becomes sufficiently large, the electrons acquire relativistic velocities, which leads to a decrease in effective plasma frequency because the electron mass depends on the electron energy. For this reason, when the nanofilm thickness is considerably smaller than the wavelength, the part of the laser pulse with a moderate intensity is reflected, whereas the high-intensity part passes through the nanofilm. Reflection to transmission switching may occur in a time comparable to the field oscillation period, and as a result the leading edge width of the resulting pulse is of the same order as or even smaller than the laser wavelength.

The reflected pulse parameters can be tuned in a wide range using plasma layers several laser wavelengths in thickness, with a density 3 to 20 times the critical one [13]. When having adequate parameters, such layers allow one to suppress almost completely the small-amplitude part of the pulse leading edge (which may be also relativistic), whereas the largest amplitude part of the pulse may pass through such layers almost with no loss. Such plasma layers can, in principle, be obtained from nanofilms using preheating laser pulses with appropriate parameters, preceding a main pulse.

The classic problem of electromagnetic field reflection from an ideal mirror was treated as early as 1905 by Einstein [14].

* Presented at the Laser Optics Conference, St. Petersburg, Russia, June 2012.

V.V. Kulagin Sternberg Astronomical Institute, M.V. Lomonosov Moscow State University, Universitetskii prosp. 13, Moscow, 119991 Russia; e-mail: victorvkulagin@yandex.ru;
V.N. Kornienko, V.A. Cherepenin V.A. Kotel'nikov Institute of Radio-Engineering and Electronics, Russian Academy of Sciences, Mokhovaya ul. 11/7, 125009 Moscow, Russia;
H. Suk Department of Physics and Photon Science, Gwangju Institute of Science and Technology, 261 Cheomdan-Gwagiro (Oryong-Dong), Buk-gu, Gwangju 500-712, Republic of Korea; e-mail: hysuk@gist.ac.kr

Received 24 October 2012; revision received 14 January 2013
Kvantovaya Elektronika **43** (5) 443–448 (2013)
Translated by O.M. Tsarev

Theoretical aspects of reflection from an electron beam in the microwave region were considered by Landecker [15]. The generation of reflected X-ray pulses using relativistic electron mirrors produced by exposing a nanofilm to an intense laser pulse was first proposed and analysed in Refs [16–18], where one-dimensional (1D) numerical modelling and analytical estimates were used to demonstrate the potential of the approach. Various aspects of reflection from relativistic electron mirrors and modifications of this configuration were examined in Refs [19–23]. Reflection from a relativistic plasma mirror containing not only electrons but also ions was considered by Esirkepov et al. [24], and X-ray generation on a mirror formed in a wake wave was investigated by Bulanov et al. [25].

There is also intense research interest in the generation of single attosecond pulses when intense laser pulses are reflected from semi-infinite targets (see e.g. Refs [26, 27]). The process is analysed in terms of an oscillating-mirror model. An attractive feature of this configuration is its simplicity: only one intense laser pulse is needed and the target thickness can be several microns or more. This configuration, however, fails to ensure sufficient control over the parameters of the reflected pulse, including the shape of its envelope and the phase difference between the carrier and envelope. Moreover, the reflected radiation contains all the harmonics of the incident pulse frequency, which requires frequency filtration for obtaining single attosecond pulses with a particular carrier frequency.

The objectives of this work are to determine the parameters of plasma layers that enable one to produce intense nonadiabatic petawatt electromagnetic pulses with a leading edge width smaller than the field period, to model the generation of relativistic electron mirrors with the use of such pulses and to investigate reflection of a counterpropagating probe pulse from the mirrors obtained. In contrast to previous work [22, 23], we consider reflection from a relativistic electron mirror situated in an accelerating laser pulse field, which ensures better reflection stability and almost constant reflectivity when the amplitude of the counterpropagating probe pulse increases up to the accelerating pulse amplitude.

2. Steepening of the leading edge of a petawatt laser pulse

In 2D simulations, we used a numerical code based on the particle-in-cell method. We considered a linearly polarised laser pulse propagating in the $+z$ direction. The laser wavelength in vacuum, λ, was 1 μm, and the dimensionless field amplitude, $a_0 = |e|E_0/(mc\omega)$ (where c is the speed of light in vacuum; ω and E_0 are the field frequency and amplitude in vacuum; and e and m are the charge and mass of an electron), was 20. The transverse electric field component, E_x, of the incident pulse is related to the transverse coordinate and time in the beam waist region by

$$E_x(x,t) = a_0 \exp\left[-\left(\frac{x-x_0}{w_0}\right)^4\right]\exp\left[-\left(\frac{t-t_0}{\tau}\right)^4\right]\sin\left(2\pi\frac{c}{\lambda}t\right), \quad (1)$$

where x_0 is the transverse coordinate of the beam centre; $w_0 = 20\lambda$ is the beam waist radius (the 1/e focal waist diameter is 40λ); $t_0 = 6\lambda/c$ is the time delay; and $\tau = 3\lambda/c$ is the 1/e pulse width. Thus, before interaction both the spatial and temporal envelopes of the pulse were super-Gaussian. The plasma layer thickness was 1.7 μm and the electron density in the plasma layer was 3.55×10^{21} cm^{-3} (3.17 times the critical density). The plasma layer was assumed to be fully ionised (estimates indicate that this assumption is satisfied at the field amplitudes used in our simulation) and the plasma was considered to be collisionless. The ion mass m_i was taken to be $1840m$.

Figure 1a shows the time dependences of the field for the incident and transmitted pulses. The amplitude of the first relativistic half-wave (near $z/\lambda \approx 24$) is of the same order as the maximum pulse amplitude. Before this instant, all half-waves have nonrelativistic amplitudes and cannot form a relativistic electron mirror. The spatial structure of a pulse with a steepened leading edge (Fig. 1b) corresponds to a part of a planar wavefront, which ensures the formation of a high-quality relativistic electron mirror. Thus, using plasma layers with an electron density two to three times the critical one, we can obtain an asymmetric nonadiabatic pulse with an amplitude of the first half-wave differing little form the maximum pulse amplitude.

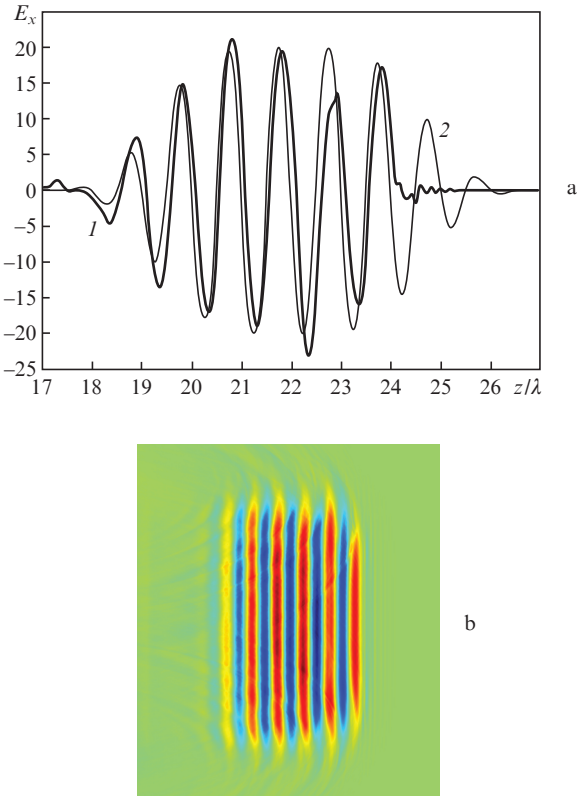

Figure 1. (a) Normalised transverse electric field component on the axis of a laser pulse as a function of longitudinal coordinate (*1*) in the presence of a plasma layer and (*2*) with no plasma. (b) Spatial structure of a pulse with a steepened leading edge.

3. Formation of a relativistic electron mirror

In addition to the laser pulse shape and amplitude, the properties (thickness and density) of the nanofilm are essential for the ability to produce a high-quality relativistic electron mirror [1, 2]. Namely, a relativistic electron mirror can be obtained at $a_0 \gg \alpha = \pi(\omega_p^2/\omega^2)(l/\lambda)$, where $\omega_p = (4\pi n_0 e^2/m)^{1/2}$ is the plasma frequency; n_0 is the electron density in the nanofilm; and l is the thickness of the nanofilm. Moreover, α influences the relative scatter in the electron energy in the mirror. For $\alpha \leqslant 1$, the scatter may be several percent, i.e. a quasi-

monochromatic electron bunch is formed [2]. In view of this, to produce a relativistic electron mirror, we used a nanofilm of thickness $l = 6$ nm, which corresponds to $\alpha \approx 0.52$ at an electron density $n_0 = 3.1\times10^{22}$ cm^{-3}.

Figure 2a shows a relativistic electron mirror produced four field periods after the onset of interaction by a pulse with a maximum amplitude $a_0 = 10$ and a steepened leading edge. At the initial instant, the nanofilm was located at $z = 3\lambda$. The thickness of the relativistic electron mirror decreases at the beginning of interaction and then increases, reaching about 15 nm at the instant corresponding to the conditions of Fig. 2. The diameter of the flat part of the mirror is 30λ, which is slightly smaller than the beam diameter (40λ). The $x-p_z$ phase space for the electrons of the mirror is shown in Fig. 2b. The mirror is seen to have good uniformity in longitudinal momentum. The average longitudinal momentum is ~43 (the momentum is normalised to mc), with a relative scatter of less than 1.5%.

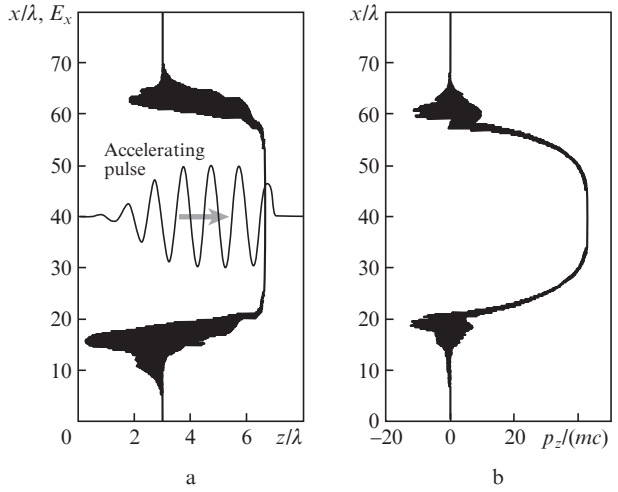

Figure 2. (a) Relativistic electron mirror produced four field periods after the onset of interaction by a pulse with a steepened leading edge and a maximum amplitude $a_0 = 10$ using a 6-nm-thick target with an electron density $n_0 = 3.1\times10^{22}$ cm^{-3}. (b) $x-p_z$ phase space for the mirror. For clarity, the field of the accelerating pulse is offset along the vertical axis.

4. Reflection of a counterpropagating probe pulse from the relativistic electron mirror formed

The reflection of a counterpropagating probe pulse from a relativistic electron mirror produced by an accelerating pulse with a steepened leading edge is illustrated by Fig. 3. A probe pulse Gaussian in shape in both the transverse and longitudinal directions has a total 1/e width of $2\lambda/c$, its amplitude is equal to the amplitude of the accelerating pulse ($a_1 = a_0 = 10$), and the beam diameter is 16λ.

The reflected pulse is similar in shape to the probe pulse. The wavelength of the reflected radiation varies from 12 to 14 nm, which is caused by the variation of the longitudinal momentum of the relativistic electron mirror in the course of its acceleration. The 1/e width of the reflected pulse is 120 as (~three oscillation periods), slightly exceeding the probe pulse width (two periods), which is caused by the comparatively large thickness (~15 nm) of the relativistic electron mirror

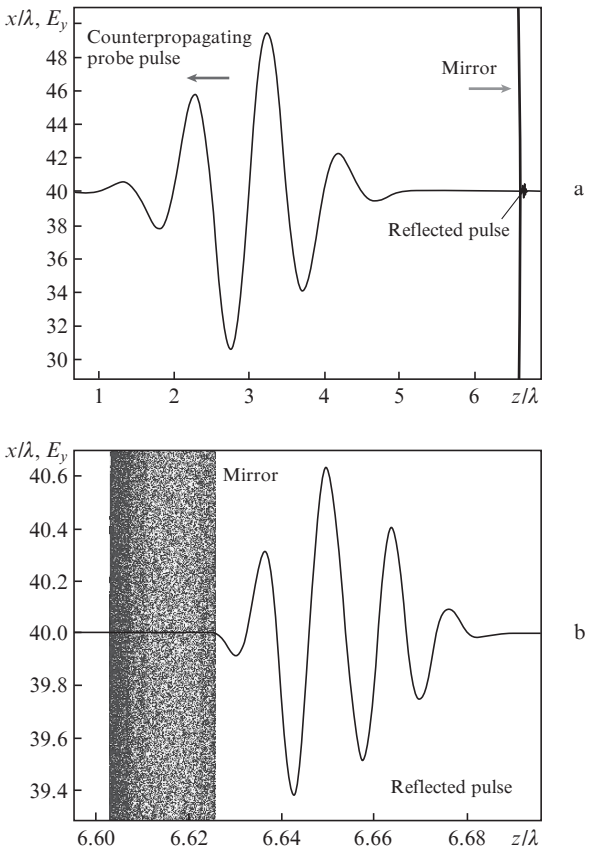

Figure 3. (a) Field of a counterpropagating probe pulse (offset along the vertical axis for clarity) on the axis of a beam of duration $2\lambda/c$ after a relativistic electron mirror and (b) field of the reflected pulse on the beam axis on an expanded scale.

at the instant of probe pulse reflection. At the instant when the largest amplitude part of the probe pulse reflects from the mirror, the increase in frequency calculated from the velocity components of the relativistic electron mirror is ~80 times, in good agreement with the wavelength of the reflected radiation.

Figure 4 shows the spatial field structure corresponding to Fig. 3, and Fig. 5 shows the reflected pulse on an expanded scale. It follows from Figs 4 and 5 that the reflected beam diameter is of the same order as the beam diameter of the probe pulse. In addition, it is seen in Fig. 5 that the reflected pulse has a well-defined spatial structure, which points to good temporal and spatial coherence.

The simulation results for the reflection of a longer pulse (1/e width of 4λ/c) from a relativistic electron mirror are pre-

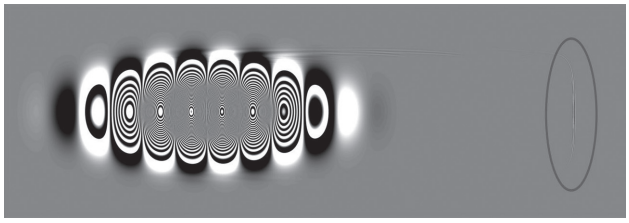

Figure 4. Spatial field structures of a counterpropagating probe pulse (left) and the reflected pulse (in the ellipse). The simulation parameters correspond to Fig. 3.

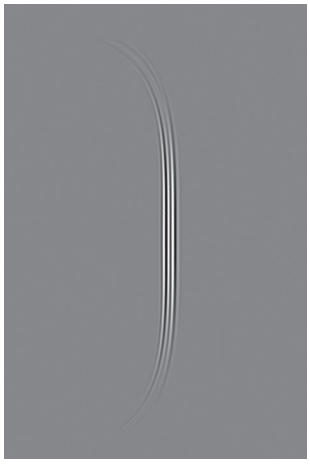

Figure 5. Spatial field structure of the reflected pulse on an expanded scale.

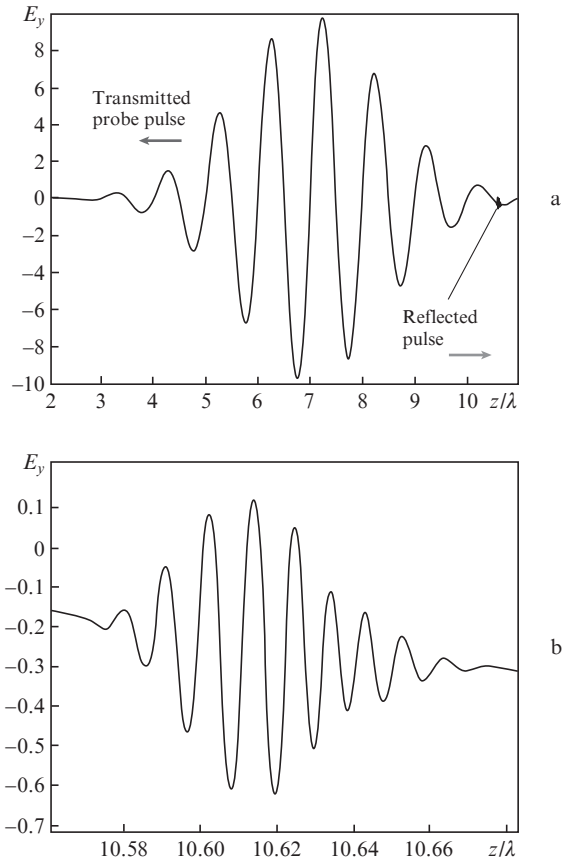

Figure 6. (a) Field of a counterpropagating probe pulse with a 1/e width of $4\lambda/c$ on the beam axis after a relativistic electron mirror and (b) field of the reflected pulse on the beam axis on an expanded scale.

sented in Fig. 6. Since the transmitted and reflected pulses are insufficiently distant from one another at the instant corresponding to the conditions of Fig. 6 (because of the limited computational resources available), the reflected pulse field is slightly tilted. In addition, the maximum amplitude of the reflected pulse is slightly smaller than that of the shorter reflected pulse (0.37 against 0.64). As for the rest, all typical features characteristic of the reflection of the shorter probe pulse (Fig. 3) remain intact.

To obtain high power of short-wavelength reflected radiation, it is important to examine the reflected pulse amplitude as a function of probe pulse amplitude (conversion nonlinearity). The reflection process was simulated for a probe pulse amplitude, a_1, varied from 0.1 to 10, that is, to the accelerating pulse amplitude. Figure 7 shows the reflected pulse amplitude and the reflectivity of the relativistic electron mirror as functions of probe pulse amplitude. The reflection process is seen to be highly linear: the reflectivity changes very little (from 0.062 to 0.064) when the amplitude of the counterpropagating probe pulse, a_1, increases from $0.01a_0$ up to the accelerating pulse amplitude, a_0. Previously, this was proved analytically in a 1D model [16].

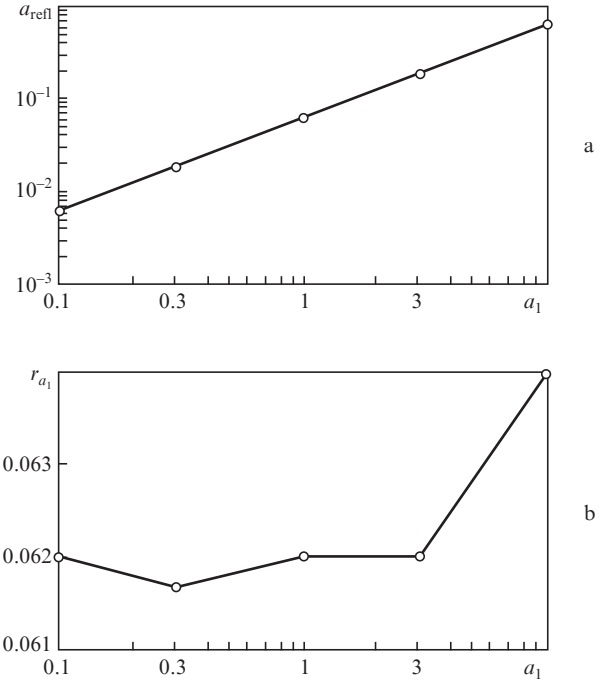

Figure 7. (a) Reflected pulse amplitude a_{refl} and (b) reflectivity of the relativistic electron mirror $r_{a_1} = a_{\text{ref}}/a_1$ as functions of probe pulse amplitude a_1.

It is worth noting that not only the reflectivity but also the shape of the reflected pulse depend little on the probe pulse amplitude. Figure 8 shows the reflected pulse field on the beam axis at counterpropagating probe pulse amplitudes differing by hundred times. The shapes of the reflected pulse are seen to be almost identical, and the slight discrepancy at the reflected pulse tail is caused by the deceleration of the relativistic electron mirror because of the influence of the counterpropagating probe pulse field and by the corresponding decrease in the frequency conversion coefficient.

5. Discussion and conclusions

The practical implementation of the above scheme for the generation of coherent attosecond X-ray pulses with tailored parameters is possible if a number of conditions are fulfilled. First, nanometre-thick targets are needed. Free-standing carbon films 5 nm or more in thickness have relatively long been used in physical experiments [28]. Graphene nanofilms can have a smaller thickness, down to the carbon monolayer

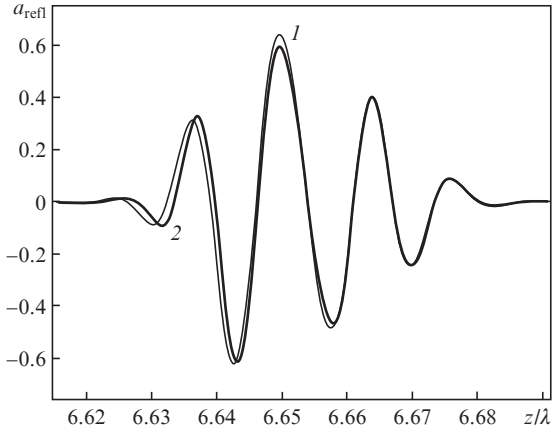

Figure 8. Reflected pulse field on the beam axis (total 1/e probe pulse width of $2\lambda/c$) at counterpropagating probe pulse amplitudes $a_1 = (1)$ 10 and (*2*) 0.1 [the vertical axis is expanded by a factor of 100 for curve (*2*)].

thickness [29–31]. In recent years, intensive research effort has been concentrated on various techniques for the preparation of carbon nanofilms through ion deposition [32]. The process used by Bai et al. [33] to fabricate a 'graphene nanomesh' allows one to produce nanofilms with an effective electron density lower than that in solids. Thus, the problem of fabricating a target possessing all necessary properties (thickness, strength, stability to disturbances and others) can be considered solved. Another condition is a rather high laser pulse contrast: up to 10^{10} or even higher. This problem is being solved using plasma mirrors transmitting the small-amplitude part of a pulse and reflecting its central part, with the maximum amplitude, because of the plasma formation on their surface. The two solutions were implemented in the first experiments concerned with the generation of relativistic electron mirrors [34], which demonstrated the formation of quasi-monochromatic electron bunches when intense laser pulses interacted with nanometre targets, and in experiments devoted to the acceleration of ions from a nanofilm [35]. At the same time, steepening of the leading edge of a laser pulse for the generation of relativistic electron mirrors has not yet been demonstrated experimentally. The above results offer the possibility of planning such experiments.

The present results allow us to estimate characteristic parameters of X-ray pulses generated when a probe pulse is reflected from relativistic electron mirrors. The data presented in Figs 3 and 4 indicate that the reflected X-ray pulse power is ~580 GW at a pulse duration of 120 as and a wavelength of 13 nm. With the same accelerating pulse, the beam diameter for a counterpropagating probe pulse can be increased to $(30–35)\lambda$, and the reflected pulse power will then reach several terawatt. The accelerating pulse power is then ~1 PW, which can be achieved in modern laser systems. The reflected pulse frequency can be raised through a reduction in the beam diameter for an accelerating pulse and the corresponding increase in beam intensity. For example, when the beam diameter for an accelerating pulse is reduced by a factor of 2–3, the reflected pulse frequency increases by a factor of 4–9 [2, 16], which allows one to obtain X-ray pulses with a wavelength of 1–2 nm. Numerical simulation of such interactions requires great computational resources and will be the subject of subsequent communications.

Thus, we have studied the generation of coherent attosecond X-ray pulses of controlled shape through the reflection of counterpropagating laser pulses from relativistic electron mirrors. We have identified conditions under which plasma layers can be used to produce an asymmetric pulse with an amplitude of the first half-wave differing little from the maximum pulse amplitude. Using 2D numerical simulation, we have investigated the generation of relativistic electron mirrors through the interaction of such pulses with nanofilms and the reflection of a counterpropagating probe pulse from such mirrors. The coherent X-ray pulses obtained have a duration of ~120 as and a power of ~580 GW at a wavelength of ~13 nm. Our results demonstrate that the reflectivity of a relativistic electron mirror situated in the accelerating pulse field is independent of the probe pulse amplitude in a wide range of its values.

Acknowledgements. This work was supported by the Russian Foundation for Basic Research (Grant Nos 11-02-12259-ofi-m-2011, 12-02-92702-IND_a and 13-02-01398_a) and the Asian Laser Center (APRI GIST, South Korea). H. Suk thanks the Korean National Research Foundation for financial support (Grant Nos 2012-0000165 and R15-2008-006-01-001-0).

References

1. Kulagin V.V., Cherepenin V.A., Hur M.S., et al. *Phys. Rev. Lett.*, **99**, 124801 (2007).
2. Kulagin V.V., Cherepenin V.A., Gulyaev Y.V., et al. *Phys. Rev. E*, **80**, 016404 (2009).
3. Bulanov S.V. *IEEE Trans. Plasma Sci.*, **24**, 393 (1996).
4. Vshivkov V.A., Naumova N.M., Pegoraro F., Bulanov S.V. *Phys. Plasmas*, **5**, 2727 (1998).
5. Kulagin V.V., Cherepenin V.A., Hur M.S., Suk H. *Phys. Plasmas*, **12**, 113102 (2007).
6. Kaw P., Dawson J. *Phys. Fluids*, **13**, 472 (1970).
7. Tushentsov M., Kim A., Cattani F., Anderson D., Lisak M. *Phys. Rev. Lett.*, **87**, 275002 (2001).
8. Lefebvre E., Bonnaud G. *Phys. Rev. Lett.*, **74**, 2002 (1995).
9. Shen B., Xu Z. *Phys. Rev. E*, **64**, 056406 (2001).
10. Goloviznin V. et al. *Phys. Plasmas*, **7**, 1564 (2000).
11. Cattani F., Kim A., Anderson D., Lisak M. *Phys. Rev. E*, **62**, 1234 (2000).
12. Eremin V.I., Korzhimanov A.V., Kim A.V. *Phys. Plasmas*, **17**, 043102 (2010).
13. Nam I.H., Kulagin V.V., Hur M.S., Lee I.W., Suk H. *Phys. Rev. E*, **85**, 026405 (2012).
14. Einstein A. *Ann. Phys. (Leipzig)*, **322**, 891 (1905).
15. Landecker K. *Phys. Rev.*, **86**, 852 (1952).
16. Kulagin V.V., Cherepenin V.A., Suk H. *Appl. Phys. Lett.*, **85**, 3322 (2004).
17. Cherepenin V.A., Kulagin V.V. *Phys. Lett. A*, **321**, 103 (2004).
18. Kulagin V.V., Cherepenin V.A., Suk H. *Phys. Plasmas*, **11**, 5239 (2004).
19. Habs D., Hegelich M., Schreiber J., et al. *Appl. Phys. B*, **93**, 349 (2008).
20. Wu H.-C., Meyer-ter-Vehn J. *Eur. Phys. J. D*, **55**, 443 (2009).
21. Qiao B., Zepf M., Borghesi M., et al. *New J. Phys.*, **11**, 103042 (2009).
22. Wu H.-C., Meyer-ter-Vehn J., Fernandez J., Hegelich B.M. *Phys. Rev. Lett.*, **104**, 234801 (2010).
23. Wu H.-C., Meyer-ter-Vehn J., Hegelich B.M., et al. *Phys. Rev. Spec. Top. Accel. Beams*, **14**, 070702 (2011).
24. Esirkepov T.Zh., Bulanov S.V., Kando M., et al. *Phys. Rev. Lett.*, **103**, 025002 (2009).
25. Bulanov S.V., Esirkepov T.Zh., Tajima T. *Phys. Rev. Lett.*, **91**, 085001 (2003).
26. Thaury C., Quere F. *J. Phys. B: At. Mol. Opt. Phys.*, **43**, 213001 (2010).

27. Heissler P., Horlein R., Mikhailova J.M., et al. *Phys. Rev. Lett*., **108**, 235003 (2012).
28. McComas D.J., Allegrini F., Pollock C.J., et al. *Rev. Sci. Instrum*., **75**, 4863 (2004).
29. Novoselov K.S., Geim A.K., Morozov S.V., et al. *Science*, **306**, 666 (2004).
30. Novoselov K.S., Jiang D., Schedin F., et al. *Proc. Natl. Acad. Sci. U.S.A*., **102**, 10451 (2005).
31. Geim A.K., Novoselov K.S. *Nat. Mater.*, **6**, 183 (2007).
32. Ma W., Liechtenstein V.Kh., Szerypo J., et al. *Nucl. Instrum. Methods Phys. Res., Sect. A*, **655**, 53 (2011).
33. Bai J., Zhong X., Jiang S., et al. *Nat. Nanotechnol*., **5**, 190 (2010).
34. Kiefer D., Henig A., Jung D., et al. *Eur. Phys. J. D*, **55**, 427 (2009).
35. Henig A., Steinke S., Schnurer M., et al. *Phys. Rev. Lett*., **103**, 045002 (2009).